High-order WCNS

ISAS, JAXA
Taku Nonomura

Chapter 1

High-order WCNS

In this document, the family of the high-order WCNS is introduced and the resolution is compared.

1.1 General Form of WCNS

Here, $(2r-1)$th order WCNS, which is expanded from the fifth order WCNS straight forwardly, is introduced. The $(2r-1)$th order WCNS consists of the $(2r-1)$th order non-linear interpolation, the flux evaluation, the $2r$th order difference scheme. In this section, the general forms of the $(2r-1)$th order non-linear interpolation and the $2r$th order difference scheme are introduced, where the flux evaluation is not discussed. In addition, the WCNS for the following generalized scalar equation is only noted here with the fifth order to ninth order coefficients computed by using MATHMATICA.[1]

$$\frac{\partial u}{\partial t} + \frac{\partial f(u)}{\partial x} = 0 \tag{1.1}$$

For the implementation to Euler equation, see the Reference[2] in which fifth-order WCNS procedure for Euler equation is described.

$(2r-1)$th order non-linear interpolation

The procedure of the interpolation from the variables u_j on the grid point to that $u^L_{j+\frac{1}{2}}$, $u^R_{j+\frac{1}{2}}$ on left side and right side of the cell center with upwinding stencils are explained. Hereafter, procedures of the construction of $u^L_{j+\frac{1}{2}}$ are only noted, while we can compute $u^R_{j+\frac{1}{2}}$ symmetrically. Following an one-point upwind biased $2r-1$ points-stencil is used in $2r-1$ th order interpolation.

$$S_{j+\frac{1}{2}} = \{x_{j-r}, x_{j-r+1}, \ldots, x_{j+r}\} \tag{1.2}$$

Then four four-point sub-stencils are constructed. kth ($k = 1, 2, \ldots, r$)) sub-stencil $S_{j+\frac{1}{2},k}$ is written as follows.

$$S_{j+\frac{1}{2},k} = \{x_{j+k-r-1}, x_{j+k-r}, \ldots, x_{j+k-1}\} \tag{1.3}$$

Then rth order interpolation with each sub-stencil is computed. In this procedure and the procedure of calculating smooth indicator discussed later, the expression using nth differential helps us to construct the algorism easily. Therefore nth differential ($n = 1, 2, \ldots, r-1$) of sth characteristic variable with using kth stencil is approximated with difference operator as follows.

$$u^{(n)}_{j+\frac{1}{2},k} = \sum_{l=1}^{r} c_{k,l} u_{j+k-r+l}, \tag{1.4}$$

where $c_{k,l}$ are the constant coefficients. $c_{k,l}$ for fifth to ninth order WCNS are shown in Tables 1.1-1.9.

Table 1.1: Coefficients $c_{1,k,l}$ in fifth-order WCNS interpolation.

	$c_{1,k,1}$	$c_{1,k,2}$	$c_{1,k,3}$
k=1	1/2	-2	3/2
k=2	-1/2	0	1/2
k=3	-3/2	2	-1/2

Table 1.2: Coefficients $c_{2,k,l}$ in fifth-order WCNS interpolation.

	$c_{2,k,1}$	$c_{2,k,2}$	$c_{2,k,3}$
k=1	1	-2	1
k=2	1	-2	1
k=3	1	-2	-1

Then rth order interpolation of the variable on cell-center with using kth stencil is written as follows.

$$u^{L}_{j+\frac{1}{2},k} = u_j + \sum_{n=1}^{r-1} \left(\frac{1}{n!}\right) \left(\frac{\Delta x}{2}\right)^n u^{(n)}_{j+\frac{1}{2},k} \tag{1.5}$$

Table 1.3: Coefficients $c_{1,k,l}$ in seventh-order WCNS interpolation.

	$c_{1,k,1}$	$c_{1,k,2}$	$c_{1,k,3}$	$c_{1,k,4}$
k=1	-1/3	3/2	-3	11/6
k=2	1/6	-1	1/2	1/3
k=3	-1/3	-1/2	1	-1/6
k=4	-11/6	3	-3/2	1/3

Table 1.4: Coefficients $c_{2,k,l}$ in seventh-order WCNS interpolation.

	$c_{2,k,1}$	$c_{2,k,2}$	$c_{2,k,3}$	$c_{2,k,4}$
k=1	-1	4	-5	2
k=2	0	1	-2	1
k=3	1	-2	1	0
k=4	2	-5	4	-1

Table 1.5: Coefficients $c_{3,k,l}$ in seventh-order WCNS interpolation.

	$c_{3,k,1}$	$c_{3,k,2}$	$c_{3,k,3}$	$c_{3,k,4}$
k=1	-1	3	-3	1
k=2	-1	3	-3	1
k=3	-1	3	-3	1
k=4	-1	3	-3	1

Table 1.6: Coefficients $c_{1,k,l}$ in ninth-order WCNS interpolation.

	$c_{1,k,1}$	$c_{1,k,2}$	$c_{1,k,3}$	$c_{1,k,4}$	$c_{1,k,5}$
k=1	1/4	-4/3	3	-4	25/12
k=2	-1/12	1/2	-3/2	5/6	1/4
k=3	1/12	-2/3	0	2/3	-1/12
k=4	-1/4	-5/6	3/2	-1/2	1/12
k=5	-25/12	4	-3	4/3	-1/4

We can obtain $2r-1$th order Lagrange interpolation of the variable on cell-center with

Table 1.7: Coefficients $c_{2,k,l}$ in ninth-order WCNS interpolation.

	$c_{2,k,1}$	$c_{2,k,2}$	$c_{2,k,3}$	$c_{2,k,4}$	$c_{2,k,5}$
k=1	11/12	-14/3	19/27	-26/37	35/12
k=2	-1/12	1/3	1/2	-5/3	11/12
k=3	-1/12	4/3	-5/2	4/3	-1/12
k=4	11/12	-5/3	1/2	1/3	-1/12
k=5	35/12	-26/3	19/2	-14/3	11/12

Table 1.8: Coefficients $c_{3,k,l}$ in ninth-order WCNS interpolation.

	$c_{3,k,1}$	$c_{3,k,2}$	$c_{3,k,3}$	$c_{3,k,4}$	$c_{3,k,5}$
k=1	3/2	-7	12	-9	5/2
k=2	1/2	-3	6	-5	3/2
k=3	-1/2	1	0	-1	1/2
k=4	-3/2	5	-6	3	-1/2
k=5	-5/2	9	-12	7	-3/2

Table 1.9: Coefficients $c_{4,k,l}$ in ninth-order WCNS interpolation.

	$c_{4,k,1}$	$c_{4,k,2}$	$c_{4,k,3}$	$c_{4,k,4}$	$c_{4,k,5}$
k=1	1	-4	6	-4	1
k=2	1	-4	6	-4	1
k=3	1	-4	6	-4	1
k=4	1	-4	6	-4	1
k=5	1	-4	6	-4	1

optimum weighted averaging of r rth order Lagrange interpolations.

$$u^L_{j+\frac{1}{2}} = \sum_{k=1}^{r} C_k u^L_{j+\frac{1}{2},k} \tag{1.6}$$

where, C_k is optimum weight. C_k of fifth to ninth order WCNS are shown in Table 1.10-1.12.

However, we have oscillations near a discontinuity with using these optimum weights. Therefore the non-linear weight w_k ,which is computed with the smooth indicator $IS_{j+\frac{1}{2},k}$, is used to obtain the weighted averaged value to suppress the numerical oscillations. In

Table 1.10: Coefficients C_k in fifth-order WCNS interpolation.

C_1	C_2	C_3
1/16	10/16	5/16

Table 1.11: Coefficients C_k in WCNS seventh-order interpolation.

C_1	C_2	C_3	C_4
1/64	21/64	35/64	7/64

Table 1.12: Coefficients C_k in ninth-order WCNS interpolation.

C_1	C_2	C_3	C_4	C_k
1/256	9/64	63/128	21/64	9/256

actual, weighted averaging is written as follows.

$$u^L_{j+\frac{1}{2}} = \sum_{k=1}^{r} w_k u^L_{j+\frac{1}{2},k}, \tag{1.7}$$

where

$$w_{j+\frac{1}{2},k} = \frac{\alpha_k}{\sum_{l=1}^{r} \alpha_l} \tag{1.8}$$

$$\alpha_{j+\frac{1}{2},k} = \frac{C_k}{{IS_k}^2 + \epsilon} \tag{1.9}$$

$$IS_{j+\frac{1}{2},k} = \sum_{n=1}^{r-1} \left(u^{(n)}_{j+\frac{1}{2},k} \right)^2. \tag{1.10}$$

ϵ is very small number to prevent zero divide. Using Eq. 1.10, w_k approaches to C_k in continuous region and Eq. 1.7 becomes the seventh order interpolation.

In this manner, $u^L_{j+\frac{1}{2}}$ is obtained.

$(2r)$th high order difference

Then $f_{j+\frac{1}{2}}$ is constructed from $u^L_{j+\frac{1}{2}}$ and $u^R_{j+\frac{1}{2}}$ with the upwind flux evaluation methods such as Roe's FDS. Using $f_{j+\frac{1}{2}}$, the high order differencing is conducted. In this document,

three types of the difference scheme, explicit, tri-diagonal compact (Implicit) and penta-diagonal compact ones, are adopted.

A general form of the high order difference scheme is written as

$$\begin{aligned}\beta_W f'_{j-2} + \alpha_W f'_{j-1} + \quad & f'_j \quad + \alpha_W f'_{j+1} + \beta_W f'_{j+2} \\ = \quad & \frac{a_W}{\Delta x}(f_{j+1/2} - f_{j-1/2}) + \frac{b_W}{\Delta x}(f_{j+3/2} - f_{j-3/2}) \\ + \quad & \frac{c_W}{\Delta x}(f_{j+5/2} - f_{j-5/2}) + \frac{d_W}{\Delta x}(f_{j+7/2} - f_{j-7/2}) \\ + \quad & \frac{e_W}{\Delta x}(f_{j+9/2} - f_{j-9/2}),\end{aligned} \tag{1.11}$$

where the coefficients of forth-order to tenth-order are written in Table 1.13.

Table 1.13: Coefficients of the generalized cell-center to cell-node difference scheme.

coefficients	α	β	a	b	c	d	e
fourth-order explicit	0	0	$\frac{9}{8}$	$-\frac{1}{24}$	0	0	0
fourth-order tri-diagonal	$\frac{1}{22}$	0	$\frac{12}{11}$	0	0	0	0
sixth-order explicit	0	0	$\frac{75}{64}$	$-\frac{25}{384}$	$\frac{3}{640}$	0	
sixth-order tri-diagonal	$\frac{9}{62}$	0	$\frac{63}{62}$	$\frac{17}{186}$	0	0	0
eighth-order explicit	0	0	$\frac{1225}{1024}$	$-\frac{245}{3072}$	$\frac{49}{5120}$	$-\frac{5}{7168}$	0
eighth-order tri-diagonal	$\frac{25}{118}$	0	$\frac{2675}{2832}$	$\frac{925}{5664}$	$-\frac{61}{28320}$	0	0
eighth-order penta-diagonal	$\frac{6114}{25669}$	$\frac{183}{51338}$	$\frac{23400}{25669}$	$\frac{14680}{77007}$	0	0	0
tenth-order explicit	0	0	$\frac{19845}{16384}$	$-\frac{735}{8192}$	$\frac{567}{40960}$	$-\frac{405}{229376}$	$\frac{35}{294912}$
tenth-order tri-diagonal	$\frac{49}{190}$	0	$\frac{12985}{14592}$	$\frac{78841}{364800}$	$-\frac{343}{72960}$	$\frac{129}{851200}$	0
tenth-order penta-diagonal	$\frac{96850}{288529}$	$\frac{9675}{577058}$	$\frac{683425}{865587}$	$\frac{505175}{1731174}$	$\frac{69049}{8655870}$	0	0

Time integration

For time integration, TVD-RK is also used in this document.

Order of Accuracy

The order of the WCNS is determined by the smaller order of the odd order accurate interpolation and the even order accurate differentiation. Thus the combination of the interpolation and the difference schemes realize the fourth to ninth order WCNS using the coefficients shown in this document. Following sections, the order of cell-center to cell-node difference s is set to be $2r$, where the order of the interpolation scheme set to be

$2r-1$. Thus the WCNS scheme becomes $(2r-1)$th order in this study. In addition, in this paper, $(2r-1)$th order WCNS is called WCNS$(2r-1)$D, where D is the differential type suffix. The suffix D can be E, T or P, which denotes explicit, tri-diagonal and penta-diagonal respectively.

1.2 Wave Resolution Using Fourier Analysis

In this section, the wave resolutions of the WCNS using Fourier analysis are investigated. Investigated schemes are WCNS5E, WCNS5T, WCNS7E, WCNS7T, WCNS7P, WCNS9E, WCNS9T, WCNS9P and the sixth order Pade type compact difference scheme as reference one. These wave resolutions are computed using ideal weights instead of non-linear weight for simplicity. The Fourier analysis is explained as follows. When

$$u_j = \exp(iwx_j) \tag{1.12}$$

is spatially differenced with the numerical method, the numerical difference u'_j is written as

$$u'_j = iw^* \exp(iwx_j). \tag{1.13}$$

$w*$ is calculated as analytically. Ideally, it is

$$w^* = w. \tag{1.14}$$

The results of this analysis are shown in Fig. 1.1. In the case of the WCNS, Imaginary parts of w^*, which represent phase-lags, exist because WCNSs are upwind schemes, in other words it is biased to one-side. Figure 1.1 shows that the modified wave numbers of the higher order WCNS are closer to the spectral (ideal) one. In other words, Fig. 1.1 shows that higher order WCNS has higher resolution. However, the difference among the explicit, tri-diagonal and penta-diagonal schemes change the modified wave number little. In addition, the real part of the modified wave number of the tri- or penta-diagonal scheme is little closer to spectral one than explicit, but the absolute value of the imaginary part of the modified wave number of the tri- or penta-diagonal scheme is larger than that of explicit one. These two effects cancel out and the resolution of tri or penta-diagonal does not seem to be different from explicit. Therefore the result shows that the type of cell-center to cell-node difference of the higher order WCNS does not change the resolution so much, as similar to the fifth order WCNS case investigated by Deng et al. Therefore the explicit scheme, which needs the smallest computational cost, is recommended as similar to the suggestion of Deng et al.

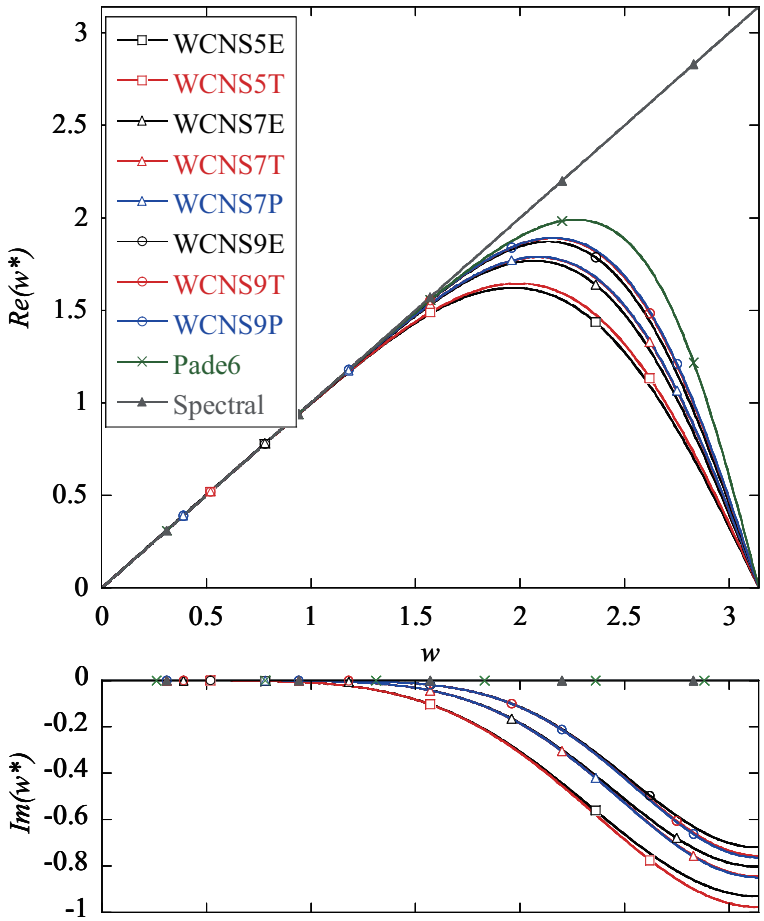

Figure 1.1: Fourier analysis of the high order WCNSs

1.3 Owo-dimensional numerical tests

One-dimensional numerical tests of the higher order WCNSs are conducted. In this section, the following one-dimensional Euler equations are computed.

$$\frac{\partial Q}{\partial t} + \frac{\partial E(Q)}{\partial x} = 0 \tag{1.15}$$

$$Q = \begin{bmatrix} \rho \\ \rho u \\ e \end{bmatrix}, \quad E = \begin{bmatrix} \rho u \\ \rho u^2 + p \\ (e+p)\,u \end{bmatrix}, \quad e = \frac{1}{\gamma - 1} p + \frac{1}{2} \rho u^2. \tag{1.16}$$

First, Sod's problem[3] is computed to verify the shock capturing ability of the higher order WCNS. Sod's problem is formulated as the initial value problem written as follows.

$$\begin{aligned} Q(x, t=0) &= \left\{ \begin{array}{l} Q_L(x \le 0) \\ Q_R(x > 0) \end{array} \right\} \\ Q_L = (\rho_L, u_L, p_L) &= (1, 0, 0) \\ Q_R = (\rho_R, u_R, p_R) &= (0.125, 0, 0.1) \end{aligned} \tag{1.17}$$

In the test case, grid points are set to be 100 and the CFL number is set to be 0.6. This problem is solved until the time t=2.0. The schemes used in the test are WCNS5E, WCNS5T, WCNS7E, WCNS7T, WCNS7P, WCNS9E, WCNS9T and WCNS9P with Lax-Fredrich flux splitting. Figure 1.2 shows the computational results where solid line shows "exact" solution, which is computed with 1600 grid points by WCNS9E. All schemes can resolve a shock wave without any numerical oscillations. On the other hand, the resolutions of these schemes are almost same because the flow-field of the problem seems to be simple.

Then the shock-entropy wave interaction problem[4] is computed to verify the resolution near the discontinuity. The problem is also formulated as the initial value problem written as follow.

$$\begin{aligned} Q(x, t=0) &= \left\{ \begin{array}{l} Q_L(x \le 4) \\ Q_R(x > 4) \end{array} \right\} \\ Q_L = (\rho_L, u_L, p_L) &= (3.857143, 2.629369, 10.3333) \\ Q_R = (\rho_R, u_R, p_R) &= (1 + 0.2\sin(0.5\pi x), 0, 1) \end{aligned} \tag{1.18}$$

Grid points used in the test is 200 points which is less points than the studies of WCNS in the past. The CFL number is set to 0.6 and the time is integrated to t=2.0. The schemes used in the test are same as Sod's problem. Figure 1.3 shows the computational results where solid line shows "exact" solution, which is computed with 1600 grid points by WCNS9E as similar to the Sod's problem. Comparing WCNS5E, WCNS7E and WCNS9E, Fig. 1.3 shows that the higher order WCNS scheme resolves the short wave of density more exactly. Thus the higher resolution can be obtained with using the higher order WCNS. On the other hand, comparing WCNS7E, WCNS7T and WCNS7P, or WCNS9E, WCNS9T and WCNS9P, Fig. 1.3 shows that resolutions of the same order schemes are almost same. Therefore Fig. 1.3 shows that the cell-center to cell-node difference schemes do not affect the resolution of WCNS so much. The tendency of the test corresponds to the Fourier analysis in the previous section. Thus the explicit scheme is recommended because the computational cost is lowest of the three.

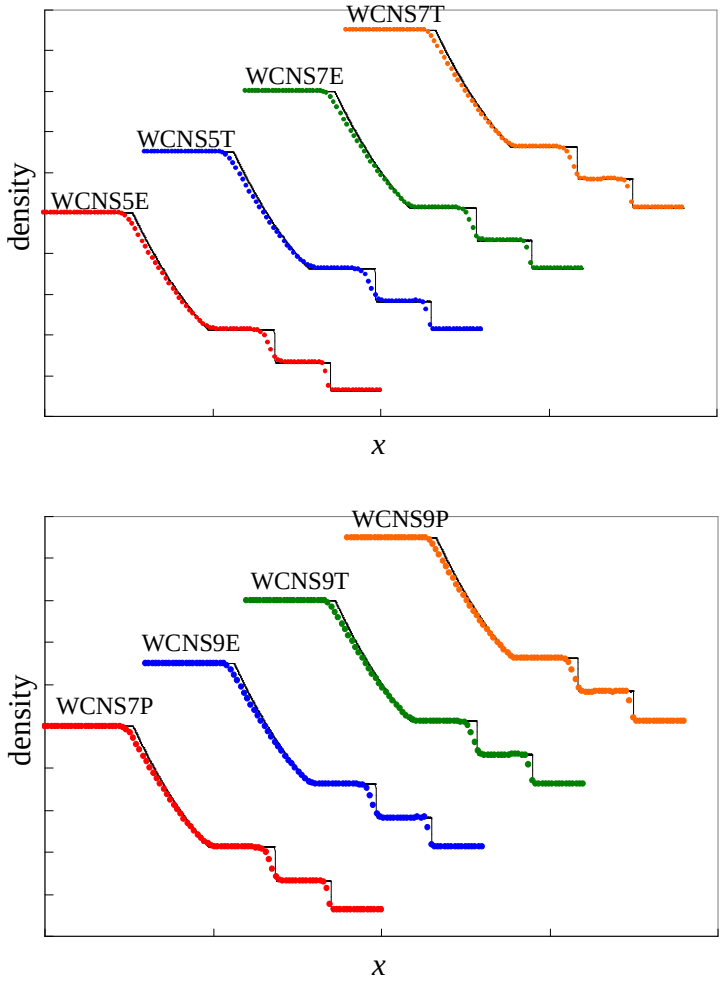

Figure 1.2: Density of Sod's problem with higher order WCNS.(solid line: exact)

1.4 Summary

The higher-order WCNSs are introduced and their resolutions are investigated analytically and numerically. First, the higher-order formulation and the coefficients of the WCNS are introduced, where the coefficients are computed with MATHEMATICA. Then the Fourier analysis of the higher order WCNS is conducted. The analysis shows that the analytical resolution of WCNS increases as the order of accuracy increases. On the other hand, the cell-center to cell-node difference scheme does not affect the analytical resolution so much. Therefore the explicit scheme is adopted in our research. Then the two one-dimensional problems, Sod's problem and the shock-entropy wave interaction problem are numerically

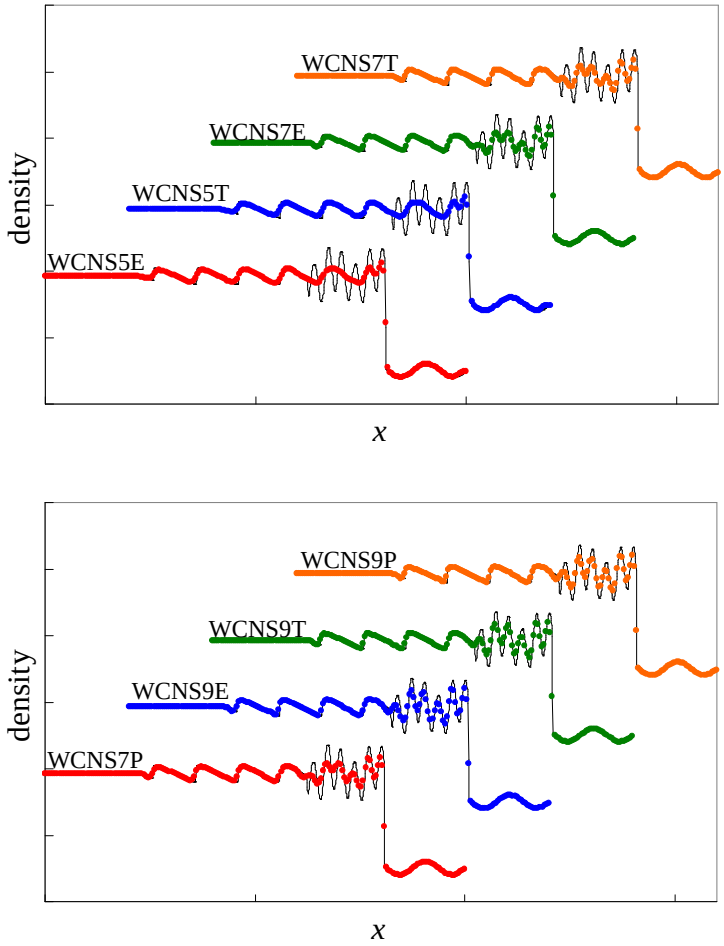

Figure 1.3: Density of Shock-Entropy Interaction problem with higher order WCNS. (solid line: exact)

examined. With regard to the Sod's problem, the WCNS schemes can resolve shock wave without any numerical oscillations. Regarding the shock-entropy wave interaction problem, the actual resolution of the WCNS increases when the high order formulation is implemented as similar to the Fourier analysis. On the other hand, the cell-center to cell-node difference scheme also does not affect the resolution well. Therefore the explicit cell-center to cell-node difference scheme, whose computational cost is the lowest, is good for the WCNS.

References

[1] URL:`http://www.wolfram.com/index.html`.

[2] Deng, X. G. and Zhang, H., "Developing High-Order Weighted Compact Nonlinear Schemes," *Journal of Computational Physics*, Vol. 165, 2000, pp. 22–44.

[3] Sod, G. A., "A Survay of Several Finite Difference Methods for Systems of Nonlinear Hyperbolic Conservation Laws," *Journal of Computational Physics*, Vol. 27, 1978, pp. 1–31.

[4] Shu, C.-W. and Osher, S., "Efficient Implementation of Essentially Non-oscillatory Shock Capturing Schemes II," *Journal of Computational Physics*, Vol. 83, 1989, pp. 32–78.